

Bioinspired economic dispatch algorithm for microgrid

Shuhan Xu^{1,*,#}, Ruoyu Tang^{2,#}, Yayu Cao³

¹Beijing Institute for Brain Research, Beijing, China

²School of Information Science and Technology, Xiamen University, Xiamen, Fujian, China

³School of Life Sciences, Xiamen University, Xiamen, Fujian, China

*Corresponding author: shuhanxu00@gmail.com, ORCID iD: 0009-0003-3838-1750

#All authors are regarded as co-first authors for the same contribution to this article

Abstract—This paper proposes a real-time economic scheduling algorithm for distributed microgrids based on bionics, combining the Sparrow Search Algorithm (SSA) with the multi-cluster reservoir Deep Echo State Network (MRDESN), to address the problems of slow response speed and insufficient accuracy of traditional iterative algorithms in complex microgrids. The algorithm simulates the behavior of sparrow colonies, optimizes network parameters through the discoverer-participant mechanism, and simultaneously adopts a hierarchical reserve pool structure to enhance the nonlinear fitting ability, achieving real-time balance of power load and power generation demand. The research constructs the MRDESN model, and utilizes SSA to optimize key parameters such as the pool size, sparsity, and spectral radius, thereby enhancing training efficiency and global search capability. The experiment takes six distributed generating units as the objects and uses the load data of North American cities to verify the performance of the algorithm. The results show that the absolute errors of the optimized SSA-MRDESN network in the two sets of test data are controlled within $\pm 0.25\text{kW}$ and $\pm 0.2\text{kW}$ respectively, the relative errors reach the order of 10^{-3} , and the mean absolute error (MAE) and root mean square error (RMSE) are significantly reduced compared with the traditional methods. This algorithm, by integrating biological bionic mechanisms with deep networks, effectively enhances the real-time performance and accuracy of microgrid dispatching, providing a new solution for economic operation in high-volatility scenarios.

Keywords—Biomimetic; Economic dispatch; Microgrid; Echo network

I. INTRODUCTION

A microgrid [1] is a small-scale power generation, distribution and consumption system [4] composed of distributed power sources [2], energy storage systems [3], energy conversion devices, monitoring and protection devices, loads, etc. At present, the dispatching systems of microgrids are divided into centralized and distributed types. A centralized system [5] refers to a system with a single allocation node, while a distributed system is a system structure that ensures the smooth operation of the system through mutual communication among nodes.

Generally, the iterative algorithm [7] is adopted to solve the economic dispatching problem of microgrids [6]. However, as the structure of microgrids becomes more complex and the volume of data increases, the iterative process of the iterative algorithm will consume more time. Since the power system requires that the power load and power generation be equal in real time, if the control signal is delayed, it will not meet the demand of the power grid. Therefore, this paper constructs a neural network model [8] to solve the economic dispatching problem of microgrids, in order to improve the response speed of controllable units and achieve real-time balance between power load and power generation. The neural network model adopted in this paper is the echo state network [8], and the data fitting effect is significantly improved by optimizing the network structure.

II. TIMELY RESPONSE ECONOMIC DISPATCH ALGORITHM FOR DISTRIBUTED MICROGRID

A. Problem description

The research content is the tertiary control in the hierarchical and graded control system [9]. Considering the power generation range and operation mode of each power generation equipment, an optimization objective is set, and the optimization objective is achieved through simulation experiments. In the fully distributed power grid studied in this paper, the processing and analysis of data are contained within each power generation equipment unit. Therefore, the simplified system structure diagram of the smart microgrid can be shown in Figure 1. The black solid line represents the power transmission line, that is, the physical layer. The dotted lines represent the information transmission lines, that is, the communication layer, and the arrows indicate the direction of signal transmission.

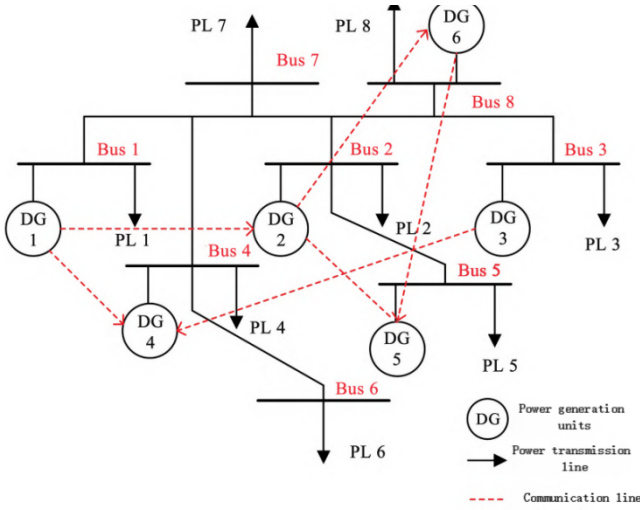


Fig. 1. Simplified diagram of the microgrid structure.

This paper studies the economic scheduling problem of microgrids. Microgrids can be represented by multi-agent systems, and the economic scheduling problem of microgrids is described as Formula (1). Among them: C represents the global power generation cost, C_i is the power generation cost of the i power generation device, x_i is the power generation capacity of the i generator, \underline{x}_i and \bar{x}_i are the upper and lower bounds of the power generation capacity of the i power generation device respectively, N is the number of power generation devices in the network, and D is the total power demand.

$$\begin{aligned} \min C &= \sum_{i=1}^N C_i(x_i) \\ \text{s.t} \quad & \underline{x}_i \leq x_i \leq \bar{x}_i \\ & \sum_{i=1}^N x_i = D \end{aligned} \quad (1)$$

Among them, the power generation cost C_i of the i power generation equipment is expressed as Equation (2) :

$$C_i(x_i) = a_i x_i^2 + b_i x_i + c_i \quad (2)$$

Among them, a_i , b_i and c_i are respectively parameters of power generation equipment, which are related to the type of power generation equipment.

B. Echo state network

ESN networks are a variant of RNN[10], consisting of an input layer, a hidden layer, and an output layer. Among them, the hidden layer is also known as the reserve pool. A large number of neurons in the reserve pool are randomly connected to store and process data. Let the number of nodes in the input layer, the reserve pool and the output layer be K , N and L respectively. At time t , the input node state, the reserve pool neuron state and the output node state of the network are respectively denoted as

$I(t) = [i_1(t), i_2(t), \dots, i_K(t)]^T$, $S(t) = [s_1(t), s_2(t), \dots, s_N(t)]^T$, $O(t) = [o_1(t), o_2(t), \dots, o_L(t)]^T$. $W^{in} \in \mathcal{R}_{N \times K}$ represents the connection weight matrix from the input layer to the reserve layer $N \times K$, $W^{res} \in \mathcal{R}_{N \times N}$ indicates the internal connection weight matrix of the reserve pool $N \times N$, and $W^{out} \in \mathcal{R}_{L \times N}$ represents the connection weight matrix from the reserve pool to the output $L \times N$. W^{in} and W^{res} remain unchanged after random initialization, while only W^{out} is obtained through supervised learning algorithm training. At time t , the update formula for the internal state of the ESN pool is Equation (3), and the update equation for the network output is equation (4) :

$$S(t) = f(W^{in}I(t) + W^{res}S(t-1)) \quad (3)$$

$$O(t) = f^{out}(W^{out}S(t)) \quad (4)$$

Here, f represents the activation function of the reserve pool neuron, and f^{out} represents the activation function of the output unit.

Advantages of the echo state network: ① Simplified training process and fast training speed; ② Strong generalization ability[11]. The specific training steps of the ESN network are as follows[12]:

Step 1: Initialization. For the given learning task, first initialize the parameters of ESN appropriately, including the number of input, reserve pool and output nodes K , N and L , as well as the connection weights W^{in} and W^{res} . Among them, W^{in} and W^{res} are random numbers that follow a uniform distribution and remain unchanged throughout the entire training and testing process. Calculate the length l_{tr} of the training samples.

Step 2: Calculate the state $S(t)$ of the reserve pool. Its calculation formula is Equation (3).

Step 3: Determine the relationship between t and l_{tr} . If $t < l_{tr}$, proceed to Step 2; If $t \geq l_{tr}$, convert to Step 4.

Step 4: Collect the status of the reserve pool and construct the reserve pool status matrix Q , as shown in Equation (5). Among them, $S(t) = [s_1(t), s_2(t), \dots, s_N(t)]$ represents the states of all the divine scripture elements in the storage pool at time t .

$$Q = \begin{bmatrix} s_1(1) & s_2(1) & \dots & s_N(1) \\ s_1(2) & s_2(2) & \dots & s_N(2) \\ \vdots & \vdots & \ddots & \vdots \\ s_1(l_{tr}) & s_2(l_{tr}) & \dots & s_N(l_{tr}) \end{bmatrix} \quad (5)$$

Step 5: Construct the expectation matrix. Collect the expected signals corresponding to the input signals at each moment and construct the expected matrix, as shown in Equation (6). Here, $d(t) = [d_1(t), d_2(t), \dots, d_L(t)]$ represents the expected output signal at time t .

$$D = \begin{bmatrix} d_1(1) & d_2(1) & \cdots & d_L(1) \\ d_1(2) & d_2(2) & \cdots & d_L(2) \\ \vdots & \vdots & \ddots & \vdots \\ d_1(l_{tr}) & d_2(l_{tr}) & \cdots & d_L(l_{tr}) \end{bmatrix} \quad (6)$$

Step 6: Calculate the output weight matrix. The objective of ESN training is to calculate W^{out} so that the actual output $O(t)$ of the network approaches the expected value $d(t)$, that is:

$$d(t) \approx O(t) = W^{out}S(t) \quad (7)$$

Therefore, its calculation method is to minimize the mean square error between $O(t)$ and $d(t)$ in the training stage, that is:

$$\min \text{MSE}_{\text{train}} = \frac{1}{l_{tr}} \sum_{t=1}^{l_{tr}} (W^{out}S(t) - d(t))^2 \quad (8)$$

This problem can be transformed into a least squares problem for solution.

C. Multi-cluster reservoir deep echo state network

The neurons of the ESN network reserve pool described in the previous text are randomly connected, which may lead to strong coupling among the neurons. Therefore, a cluster structure is constructed to solve this problem. Its structure is as follows: neurons with the same function are more closely connected, while those with different functions are more loosely connected. This section first clusters the neurons in the reservoir to construct a clustering structure network, and then builds a multi-cluster reservoir deep echo state network. The generation process of the clustered structure network and the internal weight generation process are as follows:

Step 1: Initialize the network parameters. This includes the network scale, that is, the number of neurons in the reserve pool N , the connection weight $W \in \mathbb{R}^{N \times N}$, the time window size γ , and the number of pioneer nodes, that is, the number of clusters within the reserve pool N_1 .

Step 2: Calculate the coordinates of the pioneer neurons. The specific calculation process is Equation (9). Taking the p precursor neuron as an example, $p = 1, 2, \dots, N_1$.

$$(x_p, y_p) = \left(\frac{p}{N_1+1}, 1 - \frac{p}{N_1+1} \right) \quad (9)$$

Step 3: Randomly generate neuron c whose state is $[0, 1]$.

Step 4: Calculate the connection probability P_{conn} between neuron c and the existing neurons. Take c and d as examples, the calculation formula for their connection probability is Equation (10) - Equation (11) :

$$P_{\text{conn}}(c,d) = P_{\text{dist}}(p_{cd}) \times P_{\text{time}}^{W_c}(t) \times P_{\text{time}}^{W_d}(t) \quad (10)$$

$$P_{\text{dist}}(p_{cd}) = \delta \times e^{-O \times p_{cd}} \quad (11)$$

Among them, p_{cd} is the Euclidean distance between neuron c and neuron d ; δ is the density coefficient; O is the distance coefficient; P_{dist} is the connection probability that depends on the Euclidean distance; P_{time} is the connection probability that depends on the time window.

Step 5: Randomly generate a constant $b \in (0,1)$, and compare the magnitude relationship between $P_{\text{conn}}(c,d)$ and b . If $P_{\text{conn}}(c,d) \geq b$, then establish a connection between neurons c and d and let $W(c,d) = p$, where p is the index of the precursor neuron closest to neuron c . If $P_{\text{conn}}(c,d) < b$, then neuron c is removed from the network.

Step 6: Determine the relationship between the number of neurons i and the total number N . If $i < N$, return to Step 3; Otherwise, the clustering ends.

After clustering is completed, a connection matrix W will be obtained. If there is a connection between neuron c and neuron d , then $W(c,d) = p$; If there is no connection, then $W(c,d) = 0$. According to the values of the connection matrix, after rearranging and recombining the neurons belonging to the same cluster, W can be expressed as Equation (12). The connections within the same cluster are relatively close, and as the distance increases, the connection probability decreases.

$$W = \begin{bmatrix} W_1 & & Q_1 \\ & \ddots & \\ Q_{N_1} & & W_{N_1} \end{bmatrix} \quad (12)$$

Among them, W_p is the intra-cluster connection matrix of the p cluster, and Q_p is the connection matrix between the p cluster and other clusters. The advantages of using this method are as follows: ① In clustered networks, information exchange between clusters only occurs through pioneer neurons, which can effectively reduce the coupling among a large number of neurons; ② Communication between different clusters is relatively simple, reducing the computational load of the reserve pool. ③ The clustering process can be carried out before network training, which can reduce the real-time computational load during the training process.

The ESN network [13] mentioned earlier is a single-layer network. To enhance the nonlinear fitting ability of the model [14], an MRDES network is constructed to better address the economic dispatching issue of microgrids. The network structure is shown in Figure 2. The input of the first layer of the reserve pool is the external input of the neural network, and the inputs of the other reserve pools are the outputs of the reserve pools connected to them.

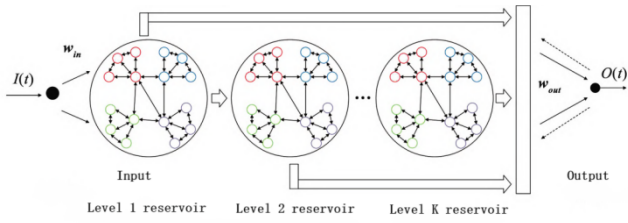


Fig. 2. Multi-cluster reservoir depth echo state network structure.

Suppose each layer of the reserve pool contains N neurons of the same number, and there are a total of K layer reserve pools. $s^{(l)} \in \mathbb{R}^N$ is the output state of the l layer of the reserve pool, where $l = 1, 2, \dots, K$. Then the output state of the first layer of the reserve pool at time t is Equation (13), where $i(t)$ is the input signal, W_{in} is the input connection matrix, W_l is the internal connection weight matrix of the l layer of the reserve pool, φ is the activation function, and $s^{(l)}(t)$ is the state of the l layer of the reserve pool at time t .

$$s^{(1)}(t) = \varphi(W_{in}^T i(t) + W_1 s^{(1)}(t-1)) \quad (13)$$

The state of the remaining reserve pools is Equation (14).

$$s^{(l)}(t) = \varphi(W_{l-1,l} s^{(l-1)}(t) + W_l s^{(l)}(t-1)) \quad (14)$$

Among them, $1 \leq l \leq K$, $W_{l-1,l}$ is the connection weight matrix between the $l-1$ layer reserve pool and the l layer reserve pool.

The final output is Equation (15).

$$O(t) = W_{out}^T S(t) \quad (15)$$

Among them, W_{out} is the output weight matrix, $S(t) = (s^{(1)}(t), \dots, s^{(K)}(t))$ is the output state matrix of all reserve pools.

The output weight matrix W_{out} , the internal link matrix W_l of the reserve pool, and the connection matrix $W_{l-1,l}$ between the reserve pools are all randomly generated. Only the output weight matrix W_{out} is obtained through training.

D. Sparrow optimization algorithm

The Sparrow Search algorithm [15] is an optimization algorithm based on the predatory behavior of sparrows. The sparrows in the population are divided into discoverers and participants. The fitness value is set in the model to distinguish the discoverer from the participant, and the one with a higher fitness value is the discoverer. A safety value is set in the model to determine whether the area is safe. When sparrows spot predators, they issue an alarm. When the alarm value is higher than the safety value, the population moves its position. The specific design concept is:

The sparrow population is shown in Equation (16) :

$$X = \begin{bmatrix} X_{11} & X_{12} & \dots & X_{1d} \\ X_{21} & X_{22} & \dots & X_{2d} \\ \vdots & \vdots & \vdots & \vdots \\ X_{n1} & X_{n2} & \dots & X_{nd} \end{bmatrix} \quad (16)$$

Here, n represents the number of sparrows, d is the dimension of the variable to be optimized, and the fitness value of the sparrows is expressed by equation (17), where f is the fitness function.

$$F_x = \begin{bmatrix} f([X_{11} & X_{12} & \dots & X_{1d}]) \\ f([X_{21} & X_{22} & \dots & X_{2d}]) \\ \vdots \\ f([X_{n1} & X_{n2} & \dots & X_{nd}]) \end{bmatrix} \quad (17)$$

The formula for the generation of dangerous sparrows is Equation (18) :

$$X_{ij}^{t+1} = \begin{cases} X_{best}^t + \beta \cdot |X_{ij}^t - X_{best}^t|, & f_i > f_g \\ X_{ij}^t + K \cdot \frac{|X_{ij}^t - X_{worst}^t|}{(f_i - f_w) + \varepsilon}, & f_i = f_g \end{cases} \quad (18)$$

Among them, X_{best} represents the current global optimal position; β is the step size control parameter, which is a random number that follows a normal distribution with a mean of 0 and a variance of 1. K is a random number and $K \in [-1, 1]$; f_i is the fitness of the i sparrow; f_g represents the current global optimal fitness. f_w represents the current global worst fitness. ε is a very small constant; Avoid situations where the denominator is zero; K is the step size control parameter, representing the movement direction of the sparrow. $f_i > f_g$ indicates that the sparrow is in a position vulnerable to attack; $f_i = f_g$ indicates that the sparrow is aware of the danger.

The discoverer has a larger search range, providing foraging directions for the population. Its position update formula is equation (19) :

$$X_{ij}^{t+1} = \begin{cases} X_{ij}^t \cdot \exp\left(-\frac{i}{a \cdot iter_{max}}\right), & R_2 < ST \\ X_{ij}^t + Q \cdot L, & R_2 \geq ST \end{cases} \quad (19)$$

Here, t represents the number of iterations, $j = 1, 2, \dots, d$, $iter_{max}$ represents the maximum number of iterations, and X_{ij} indicates the position information of the i sparrow in the j dimension. $a \in (0, 1]$ is a random number, $R_2 \in [0, 1]$ represents a warning value, and $ST \in [0.5, 1]$ represents a safety value. Q is a random number that follows a normal distribution. L represents a $1 \times d$ matrix where all elements are 1. $R_2 < ST$ indicates that the foraging environment is safe. $R_2 \geq ST$ indicates that sparrows have issued an alarm and the population needs to be transferred.

The responsibilities of the participant: To detect

predators, issue warnings, and search for foraging directions to enhance their own adaptability and join the discoverer. The position update formula is Equation (20) :

$$X_{ij}^{t+1} = \begin{cases} Q \cdot \exp\left(\frac{X_{\text{worst}} - X_{ij}^t}{i^2}\right), & i > \frac{n}{2} \\ X_p^{t+1} + |X_{ij}^t - X_p^{t+1}| \cdot A^+ \cdot L, & i \leq \frac{n}{2} \end{cases} \quad (20)$$

Among them, X_p is the current optimal position occupied by the discoverer, and X_{worst} is the global worst position. A is $1 \times d$ matrix with all elements being 1 or -1, and it satisfies $A^+ = A^T(AA^T)^{-1}$, $i > \frac{n}{2}$ indicates that the i entrant has a low fitness and is in a state of hunger, requiring a position update.

E Correction of the value of small mismatch between generation and demand

The universal approximation law of neural networks: For any continuous function $f(\cdot): \mathbb{R}^n \rightarrow \mathbb{R}^m$, a neural network with a sufficient number of neurons can make Equation (21) hold on a compact set $\Omega_z \subset \mathbb{R}^n$.

$$\sup_{z \in \Omega_z} \|f(\cdot) - y_{\text{out}}(z)\| \leq \varepsilon \quad (21)$$

Among them, $z \in \mathbb{R}^n$ is the input signal of the neural network; $y_{\text{out}}(z) \in \mathbb{R}^m$ is the output of the neural network; ε is a normal book. Therefore, $f(\cdot)$ can be further expressed as:

$$f(\cdot) = (w^*)^T h(z) + \varepsilon^* \quad (22)$$

Here, $\varepsilon^* \in \mathbb{R}^m$ represents the approximation error. When the number of neurons N in the hidden layer of the neural network is sufficient, the approximation error can be arbitrarily small and satisfy $\|\varepsilon^*\| \leq \varepsilon$, $w^* \in \mathbb{R}^N$ is the optimal output weight, that is:

$$w^* = \arg \min_{w \in \mathbb{R}^N} \left\{ \sup_{z \in \Omega_z} \|f(z) - w^T h(z)\| \right\} \quad (23)$$

Theoretically, neural networks can fit any function. However, in practical operation, due to the limited number of neurons in the hidden layer and the imperfect weight setting function and other conditions, there are often errors in their fitting. In this chapter, the error correction method is adopted to correct the fitted data. The specific method is as follows:

Step 1: Calculate the global mismatch value $\delta(n)$ of the microgrid. The calculation formula is Equation (24) :

$$\delta(n) = \frac{\sum_{i=1}^N P_i^*(n) - P_d}{N} \quad (24)$$

Here, n represents the number of iterations; N represents the number of power generation devices; P_i^* represents the network fitting optimal

power generation of the i power generation device. P_d represents the total electricity demand.

Step 2: Iterate over P_i^* . The iteration steps are as shown in Equation (25) :

$$P_i^*(n+1) = P_i^*(n) + \delta(n) \quad (25)$$

Step 3: Consider the power generation constraint, namely Equation (26) :

$$P_i^*(n+1) = \begin{cases} P_i^{\max} & P_i^*(n+1) > P_i^{\max} \\ P_i^*(n+1) & P_i^{\min} \leq P_i^*(n+1) \leq P_i^{\max} \\ P_i^{\min} & P_i^*(n+1) < P_i^{\min} \end{cases} \quad (26)$$

Step 4: Determine the relationship between the error $\delta(n)$ and 0. If $\delta(n) > 0$, return to Step 1; otherwise, proceed to Step 5.

Step 5: Output the corrected optimal power generation. Let the final number of iterations be n_s times, then $P_i^* = [P_1^*(n_s), P_2^*(n_s), \dots, P_N^*(n_s)]$.

III. EXPERIMENT AND ANALYSIS

A. Experimental setup

To facilitate the verification of the accuracy of network data, the selected microgrid topology is shown in Figure 3.

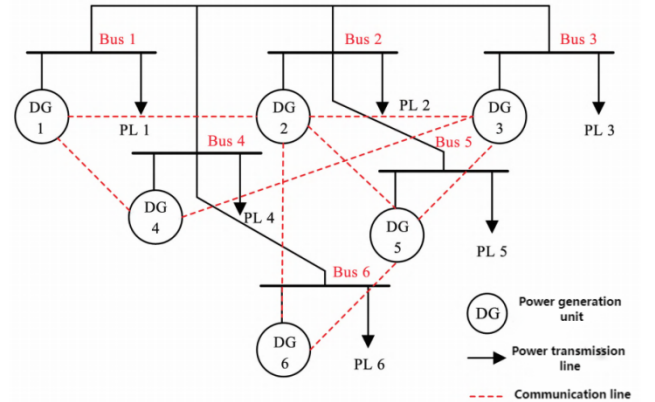


Fig. 3. Case simulation microgrid topology diagram.

The parameters of the six power generation devices in Figure 3 are shown in Table 1. Among them, α_1 , β_1 and γ_1 are the parameters in the power generation cost coefficient respectively, and P_i^{\max} and P_i^{\min} are the maximum and minimum power generation of the i power generation equipment respectively.

TABLE I. SIMULATION CASE: PARAMETERS OF POWER GENERATION EQUIPMENT.

DG	1	2	3	4	5	6
α_1 [\$/kW ² h]	-37.5	-17.5	-62.5	-83.4	-25	-0.25
β_1 [\$/kWh]	2	1.75	1	3.25	3	3
γ_1 [\$/h]	0	0	0	0	0	0
P_i^{\min} [kW]	0	0	0	0	0	0
P_i^{\max} [kW]	120	100	50	35	80	40

The load data required for training adopts two sets of data from two cities A and B in North America. Each set of data has 1,000 data points. The first 70% is used as the training set and the last 30% as the test set[16].

B. Parameters optimized by SSA

The parameters optimized in this SSA are: the scale of the reserve pool N, the sparsity α of the internal connection weight matrix of the reserve pool, and the spectral radius ρ of the internal connection weight matrix of the reserve pool. To verify the generalization ability of the model, only one parameter optimization was conducted in this experiment. The final optimization results are as follows: the pool size $N = 532$, the sparsity $\alpha=0.03$ of the internal connection weight matrix of the pool, and the spectral radius $\rho=0.02$ of the internal connection weight matrix of the pool. Parameter Settings for the SSA algorithm: The population size is 10, the maximum number of iterations is 10, and the dimension is 3, namely the pool size N, the sparsity α of the internal connection weight matrix of the pool, and the spectral radius ρ of the internal connection weight matrix of the pool. The warning value is 0.6, the proportion of discoverers is 0.7, and the proportion of sparrows sensing danger is 0.2.

C. Evaluation index

The evaluation indicators adopted in this paper mainly include the following types. Among them, the absolute error and relative error are plotted, and the other evaluation indicators are calculated. Plot and calculate the six power generation devices in each set of data respectively. In the formula, P_A represents the actual load, P_F represents the predicted load, and N represents the number of data.

Absolute Error (AE):

$$\delta_{AE} = |P_A - P_F| \quad (27)$$

Relative error (RE):

$$\delta_{RE} = \frac{|P_A - P_F|}{P_A} \quad (28)$$

Mean Absolute Error (MAE):

$$\delta_{MAE} = \frac{1}{N} \sum_{i=1}^N |P_{Ai} - P_{Fi}| \quad (29)$$

Average relative error (MRE):

$$\delta_{MRE} = \frac{1}{N} \sum_{i=1}^N \frac{|P_{Ai} - P_{Fi}|}{P_{Ai}} \quad (30)$$

Mean Square Relative Error (MSRE):

$$\sigma_{MSRE} = \sqrt{\frac{1}{N} \sum_{i=1}^N \left(\frac{|P_{Ai} - P_{Fi}|}{P_{Ai}} \right)^2} \quad (31)$$

D. Simulation analysis of economic dispatch of microgrid based on SSA-MRDESN model

Figure 4 shows the fitting error of the SSA-

MRDESN network for the first set of data. Figure 4 (a) shows the absolute error of the output power of each power generation device. From the figure, it can be seen that most of the errors are within (-0.25, 0.25) kW, the data fluctuation between 250 and 275 has intensified, but the maximum error does not exceed 1kW, and the fluctuation of the error has increased. Figure 4 (b) shows the relative errors of the output power of each power generation equipment, all of which are at the order of 10^{-3} . The fitting situation is good and the changing trend is similar to that of the absolute error. The other evaluation indicators for fitting the first set of data are $MAE = 4.25 \times 10^{-3}$, $MRE = 5.25 \times 10^{-5}$, $RMSE = 0.17022$. The data of the evaluation indicators has declined. From the perspective of evaluation indicators, the data fitting effect is relatively good, but from the perspective of data volatility, the fitting effect has decreased somewhat.

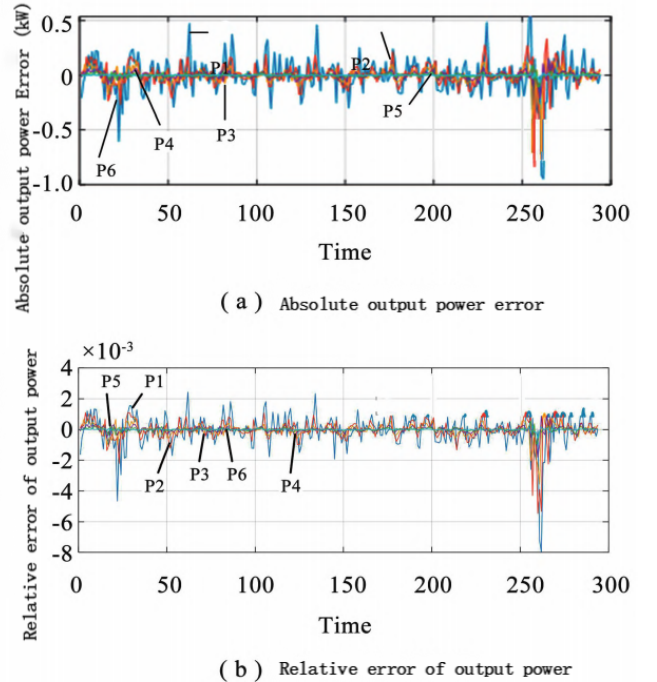


Fig. 4. A city of SSA - ESN network fitting error.

Figure 5 shows the fitting error of the SSA-MRDESN network for the second set of data. Figure 5 (a) shows the absolute error of the output power of each power generation device. From the figure, it can be seen that most of the errors are within (-0.2, 0.2) kW, it is reduced by 0 compared with part D 0.3kW. The absolute value of 0.6kW has decreased by 0 compared to part D 0.4kW. Therefore, it can be considered that the fitting effect has been improved. From the perspective of power generation equipment, the absolute value of the error of power generation equipment 1 is still significantly larger than that of other power generation equipment. Considering that the power generation range of power generation equipment P_1 is larger, the variation range of the absolute error is also larger. Figure 5 (b) shows the relative errors of the optimal output power of each

power generation equipment, all of which are at the 10^{-3} level. This indicates that the SSA-MRDESN network fits the second set of data well, similar to the changing trend of the absolute error. The relative error of P_1 is relatively large. Other evaluation indicators for the optimal power generation fitting of the second group of data are $MAE=6.622 \times 10^{-3}$, $MRE=6.23 \times 10^{-5}$, $RMSE=0.10569$, compared with part D, there is a significant decrease. In conclusion, it can be considered that the improved ESN network optimized by SSA has significantly enhanced the fitting effect of the optimal power generation for the second set of data.

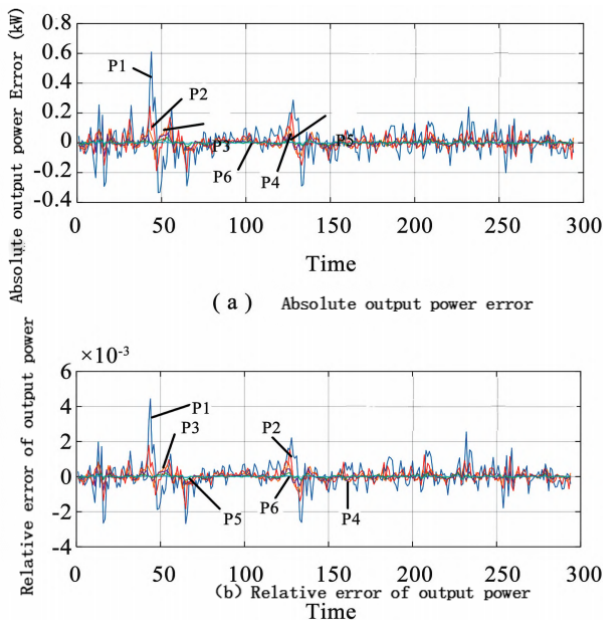


Fig. 5. B city improved SSA-ESN network fitting error.

IV. CONCLUSION

To enhance the dispatching effect of distributed microgrids, this paper studies an economic dispatching algorithm for distributed microgrids with timely response based on bionics. This performance is based on bionic algorithms and designs a multi-cluster reserve pool deep echo state network. Combined with the bionic sparrow search algorithm, a scheduling algorithm is designed. Meanwhile, through experimental analysis, it can be concluded that the SSA-MRDESN network with parameter correction by SSA plays a role in improving accuracy and has a significant effect in reducing error volatility. Therefore, the accuracy of data fitting for data groups with high volatility can be improved through parameter correction.

REFERENCES

[1] Colombo G C ,Miraftabzadeh M S ,Longo M .Powering future urban transport: a renewable-based electrification model for public transit - A Mediterranean case study[J].Energy,2025,341139375-139375.DOI:10.1016/J.ENERGY.2025.139375.

[2] Wu L ,Shao T ,He Y , et al.Economic operation optimization study of farm biogas-photovoltaic distributed generation system[J].Energy,2025,341138966-138966.DOI:10.1016/J.ENERGY.2025.138966.

[3] Chen Y ,Bao A ,Wu D , et al.Experimental study of discharge performance of pumped thermal energy storage system based on organic Rankine cycle[J].Energy,2025,340139398-139398.DOI:10.1016/J.ENERGY.2025.139398.

[4] Li Y .Effects and mechanisms of intelligent electricity system on urban carbon reduction[J].Energy Economics,2024,139107886-107886.DOI:10.1016/J.ENERGY.2024.107886.

[5] Bhatia A ,Triolo E ,Williams T L , et al.Sodium (^{23}Na) MRI in Pediatric Central Nervous System Tumors.[J].Neuroimaging clinics of North America,2026,36(1):197-208.DOI:10.1016/J.NIC.2025.09.002.

[6] Mohammadi M ,Alisher B S ,Allaberganova M , et al.Multi-Level Technical and Economic Power Scheduling in an Electrical Distribution Grid Considering the Smart Multi-Performance of the Demand Side[J].Engineering Reports,2025,7(11):e70485-e70485.DOI:10.1002/ENG2.70485.

[7] Mao J ,Li Z ,Li D , et al.A PDEM-based synchronous iterative algorithm for random vibration analysis of high-speed maglev train-bridge system[J].Journal of Sound and Vibration,2026,623119541-119541.DOI:10.1016/J.JSV.2025.119541.

[8] Zhou X ,Pan Y ,Qin J , et al.Large language model-enhanced graph neural network for quantile prediction of railway track settlement near deep excavations[J].Advanced Engineering Informatics,2026,69(PD):104105-104105.DOI:10.1016/J.AEI.2025.104105.

[9] Xu H ,Yang L .Retraction Note: Enhancing Financial Risk Prediction Through Echo State Networks and Differential Evolutionary Algorithms in the Digital Era[J].Journal of the Knowledge Economy,2025,(prepublish):1-1.DOI:10.1007/S13132-025-02991-4.

[10] An Z ,Lv S ,Yin N , et al.Research on Coordinated Control and Hierarchical Partition Control Strategy of Distributed Generation in New Power System[J].Journal of Physics: Conference Series,2024,2774(1):DOI:10.1088/1742-6596/2774/1/012050.

[11] Liu X ,Mei R ,Zhao Z , et al.An Optimized Port Operation Efficiency Prediction Model Based on ESN and LSTM[J].Journal of Software Engineering and Applications,2025,18(10):413-426.DOI:10.4236/JSEA.2025.1810025.

[12] Lu Y ,Winkler R J .Regularisation and the least squares problem in the analysis of echo state networks[J].Physica Scripta,2025,100(11):116009-116009.DOI:10.1088/1402-4896/AE082F.

[13] Joo Y ,Kim D ,Noh Y , et al.Performance Comparison of LSTM and ESN Models in Time-Series Prediction of Solar Power Generation[J].Sustainability,2025,17(19):8538-8538.DOI:10.3390/SU17198538.

[14] Xia Z ,Huang B ,Zhu C .Hierarchical RL-ESN control for autonomous underwater vehicle: 6-DOF large angle rotation maneuvering.[J].ISA transactions,2025,166393-404.DOI:10.1016/J.ISATRA.2025.07.036.

[15] Zhu W ,Zhao C .The assessment method of lip closure ability based on sEMG nonlinear onset detection algorithms.[J].Biomedizinische Technik. Biomedical engineering,2024,69(6):597-608.DOI:10.1515/BMT-2024-0107.

[16] Lu P ,Gu Z ,Jin T , et al.Bridge Structural Reliability Analysis Method Based on Kriging Model Optimized by Improved Sparrow Search Algorithm[J].International Journal of Structural Stability and Dynamics,2025,(prepublish):DOI:10.1142/S0219455427501227..